Performance of Ti/Pt and Nb/BDD anodes for dechlorination of nitric acid and regeneration of silver(II) in a tubular reactor for the treatment of solid wastes in nuclear industry

K. Groenen Serrano[1] · A. Savall[1] · L. Latapie[1] · Ch. Racaud[2] · Ph. Rondet[2] · N. Bertrand[3]

Abstract One of the problems frequently encountered in the processing of nuclear fuels is the recovery of plutonium contained in various solid wastes. The difficulty is to make soluble the plutonium present as the refractory oxide PuO_2. The dissolution of this oxide in nitric acid solutions is easily performed by means of silver(II) a strong oxidizing agent which is usually electrochemically generated on a platinum anode. However, certain solid residues that must be treated to separate actinides contain important quantities of chloride ions that require after dissolution in nitric acid a preliminary electrochemical step to be removed before introducing Ag(I) for Ag(II) electrogeneration. Research is conducted to find electrocatalytic materials being able to replace massive platinum in view to limit capital costs. In the present work a set-up including a two-compartment tubular reactor with recirculation of electrolytes was tested with anodes made of boron doped diamond coated niobium (Nb/BDD) and platinum coated titanium (Ti/Pt) grids for the removal of chlorides (up to 0.1 M) and for silver(II) regeneration. The study showed that these two anodes are effective for the removal of chlorides contained in 6 M HNO_3 solution as gaseous chlorine, without producing the unwanted oxyanions of chlorine. Furthermore, the regeneration rate of silver(II) on Nb/BDD anode is approximately equal to that obtained on Ti/Pt anode for the same hydrodynamic conditions in the tubular reactor. Accordingly, dechlorination as well as silver(II) regeneration can be performed in the same reactor equipped either with a Nb/BDD or a Ti/Pt anode. Besides, the service life of Nb/BDD anodes estimated by accelerated life tests conducted in 6 M HNO_3 can be considered as very satisfactory compared to that observed with Ti/Pt anodes.

Keywords Silver(II) · Boron doped diamond · Electrolysis · Tubular reactor · Nuclear wastes · Electrode service life

1 Introduction

Silver(II) is a strong oxidising agent ($E° = 1.98$ V/SHE) capable of attacking many organic and inorganic substances. Electrochemical processes involving Ag(II) regeneration in nitric acid solution containing silver nitrate have been developed to treat transuranic wastes [1 5] and for the safe low-temperature destruction of a wide variety of contaminated organic waste materials [6, 7]. In particular, silver(II) generated by anodic oxidation is a method of choice for the dissolution of plutonium oxide PuO_2 [1, 3, 8]:

$$PuO_{2(solid)} + 2\ Ag^{2+} \rightarrow (PuO_2)^{2+}_{(solution)} + 2\ Ag^{+}$$

Dissolution of PuO_2 is of considerable interest as this process is used in (i) aqueous reprocessing of uranium plutonium fuel, (ii) fuel fabrication by reconversion of weapons-grade Pu, and (iii) regeneration of Pu from several types of residues produced during conversion processes [3, 8]. But during some of these stages, pyrochemical processes used to recover and purify Pu metal generate ashes rich in chloride salts. Consequently, in the silver(II) process operated by the nuclear industry,

✉ A. Savall
savall@chimie.ups tlse.fr

[1] Laboratoire de Génie Chimique, Université de Toulouse, CNRS, 31062 Toulouse, France

[2] AREVA NP, 25 avenue de Tourville, 50120 Equeurdreville, France

[3] AREVA NC, 1 place Jean Millier, 92400 Courbevoie, France

chlorides contained in solid wastes must be first eliminated before dissolving PuO_2 by chemical attack of Ag(II) in nitric acid solution [8]. Indeed, the presence of chloride ions leads to the precipitation of Ag(I) cations to form AgCl, thus making impossible the regeneration of Ag(II) by electrolysis.

Although a chemical process of chloride removal from pyrochemical residues by sparging nitrogen dioxide in the solution was proposed by Pierce et al. [9], the implementation of an electrochemical process involving direct chloride oxidation can be considered as a simpler technique [8, 10]:

$$2\ Cl^- \rightarrow Cl_{2(gas)} + 2\ e^- \quad (E^\circ = 1.359\ V/SHE) \qquad (1)$$

Thus, in the process of PuO_2 dissolution it would be convenient to use the same electrochemical reactor to first eliminate chloride as gaseous chlorine by electrolysis before adding silver nitrate for the dissolution of PuO_2 by regenerating Ag(II).

In a previous study, we showed that the Nb/BDD anode can efficiently generate silver(II) in 6 mol L^{-1} nitric acid solution: compared with platinised electrodes (Ti/Pt 2 and 5 μm and Nb/Pt 5 μm), the generation speed of Ag(II) was very similar and the conversion rate was of the same order of magnitude [11]. In order to use the same anode material to perform the sequential electrochemical steps, the study of anodic chlorine evolution on BDD in nitric acid at 6 mol L^{-1} was undertaken in a tubular reactor. This typical design is suitable for an electrochemical cell with separated cathodic and anodic compartments requiring a diaphragm with good mechanical and chemical resistance; it benefits indeed from a good experience feedback in nuclear industry [3, 10].

This attempt is based on the recognized stability and the high oxygen overpotential of diamond electrodes making them excellent candidates for chlorine evolution from dilute chloride solution [12]. In fact, Ferro et al. [12] have shown by comparison of current potential curves for chlorine and oxygen evolution that under the same acidic condition (pH 3.5) the faradaic yield for chlorine evolution was very high on BDD anode. However, oxidation of chloride ions on diamond can form the undesirable chlorate and perchlorate anions [13 15]. Although these last observations were made in neutral or alkaline solutions, it was necessary to test if these unwanted products were capable of being formed under electrochemical dechlorination conditions in concentrated nitric acid.

This paper presents kinetic studies conducted in a tubular reactor to perform (i) the electrochemical dechlorination of 6 mol L^{-1} nitric acid solutions containing chloride at concentration up to 0.1 mol L^{-1} and (ii) the silver(I) oxidation at initial concentration of 0.1 mol L^{-1}. In addition, the service life of Nb/BDD anodes was estimated by accelerated life tests in nitric acid at 6 mol L^{-1}. The main objective was to test the performance of the promising Nb/BDD anode and to compare it to that of Ti/Pt.

2 Materials and methods

2.1 Electrochemical reactor

Dechlorination tests were performed under galvanostatic condition in a proprietary electrolysis set-up designed according to sub-critical geometry requirement (Fig. 1); such a geometry does not have the ability to sustain a fission chain reaction what gives security for the operators during the treatment of plutonium dioxide. Electrolyses were achieved in a tubular reactor consisting of two coaxial compartments separated by a porous ceramic diaphragm [8]. The anodic compartment was a temperature-controlled cylinder made of glass. The cathode, in the central compartment was made of stainless steel (47 cm^2). Two anodes of quasi-cylindrical shape formed by 8 rectangular plates made of expanded titanium or expanded niobium, covered by a layer of Pt (5 μm) or BDD (1 μm) respectively, were tested. Plates made of Ti/Pt were supplied by MAGNETO special anodes B.V. (NL) while the ones made of Nb/BDD were supplied by Condias GmbH (DE). Assuming that for an expanded metal both faces are equipotential, the active surface of these two electrodes was 521 cm^2. Every plate was welded on its width to a clamping collar made of the same metal, and was linked to the electrical connector across the lid (Teflon) of the reactor. At the bottom of the reactor, at the anolyte inlet, these plates were mechanically fixed to the base of a cone (Teflon). In the upper part of the reactor the clamping collar was also used to maintain the cylindrical ceramic separator. The cell was connected to a direct current supply (Delta Elektronika BV SM 52 V-30A; NL).

The cell (Fig. 1) was connected in its upper part by a glass pipe with a temperature-regulated glass tank containing 1.5 L of 6 mol L^{-1} HNO_3 solution. The anolyte was recirculated at a flow rate up to 25 L min^{-1} to ensure a satisfactory renewal of the boundary layer over the full length of the anode. Chlorine evolved in the anodic compartment was trapped in three scrubbers placed in series and containing 5 mol L^{-1} NaOH and 0.05 mol L^{-1} Na_2SO_3. The atmosphere above the cathodic compartment was swept by a flow of air to trap nitrogen dioxide formed by the complex mechanism of reduction of the concentrated nitric acid (13.6 mol L^{-1}) used as catholyte [16]. At this high concentration there is no hydrogen evolution during HNO_3 reduction that makes safe the process.

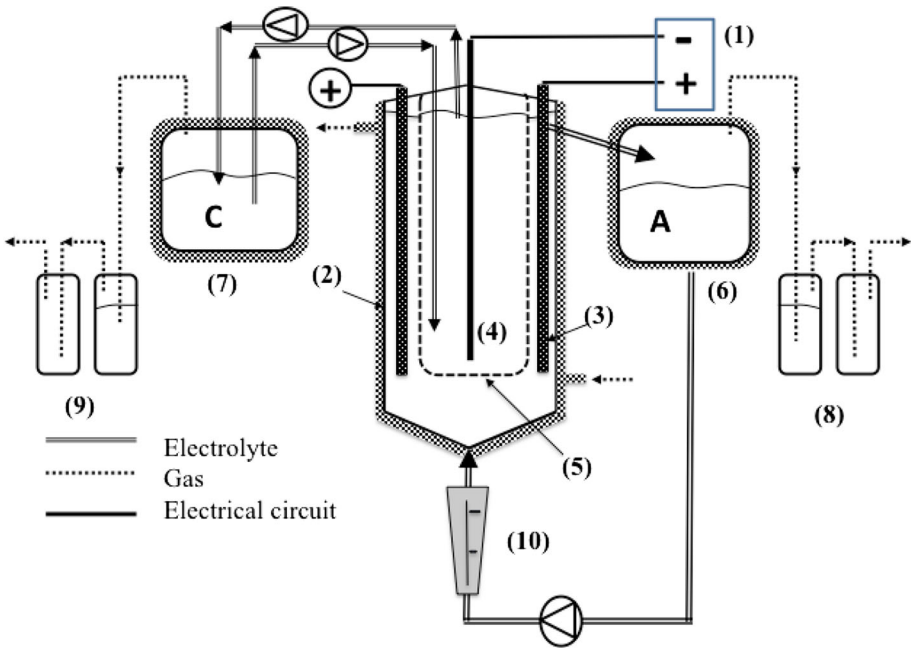

Fig. 1 Dechlorination set up. *1* Power supply *2* thermoregulated tubular reactor *3* anode (Nb/BDD or Ti/Pt) *4* cathode (SS) *5* diaphragm *6* tank (anolyte) *7* tank (catholyte) *8* chlorine absorber *9* NOx absorber *10* flowmeter

2.2 Chemicals and analysis procedure

Nitric acid 68 % (VWR, AnalaR Normapur®) was used to prepare electrolytic solutions, whereas sodium chloride and silver nitrate (Acros Organics, ACS reagent 99 %) were used as model of chloride salt for the dechlorination tests and for the electrogeneration of Ag(II) respectively.

Before each dechlorination experiment the anolyte (1.5 L of 6 mol L^{-1} HNO_3 + 0.1 mol L^{-1} NaCl) was re-circulated between the anodic compartment and the reservoir during 1 h to reach a stationary temperature of 60 °C. Samples of the anolyte taken before starting and regularly during dechlorination experiments were immediately diluted with pure water (1v/100v) in reason of the high concentration of nitric acid. Chloride, chlorate and perchlorate were analysed by ionic chromatography using a Dionex column (ICS3000, IonPac® AS19, 4 × 250 mm) and a conductometric detection. The flow rate of the pump was set to 1.0 mL min^{-1}. The mobile phase composition was constant (80 % of NaOH 5 mmol L^{-1} + 20 % of NaOH 100 mmol L^{-1}) for 1 min and then the gradient was from 20 to 90 % of NaOH 100 mmol L^{-1} during 27 min to provide good separation of all the peaks in a single chromatogram. The time to return to initial conditions was 4 min.

The end-point of electrochemical dechlorination was detected by a potentiometric titration with a constant imposed current intensity between two indicator platinum electrodes (0.28 cm^2 each). In the region of the end-point, when the concentration of chloride reaches a value lower than 10^{-3} mol L^{-1}, the potential difference ΔE between the electrodes varies considerably for an applied current intensity. This sharp change of ΔE (750 mV) which marks exactly the end of the electrolysis arises when the oxidation limiting current of Cl^- becomes lower than the applied intensity equal to 50 μA.

Silver(II) forms a brown complex (Eq. 7) in 6 mol L^{-1} nitric acid which was continuously titrated by UV Visible spectroscopy thanks to an immersed probe (Hellman; λ = 580 nm) placed in the glass tube connecting the exit of the anode compartment with the reservoir of anolyte. The probe was standardized by back potentiometry with cerium(III) nitrate hexahydrate and Mohr's salt (Acros Organics, 99.5 and 99 % respectively) as described in [11]. The rate of generation of Ag(II) was measured by considering the variation of its concentration during the first 5 min of electrolysis. The rate obtained by extrapolation at t = 0 corresponds to the maximal rate of regeneration of Ag(II) for a set of given operating conditions.

2.3 Stability of electrodes

Ageing tests were performed in a test bench composed of six electrochemical cells of 100 mL capacity, without separator, thermo-regulated at 30 °C, under agitation and with zirconium cathode (7 cm^2). The samples were submitted to galvanostatic runs in 6 mol L^{-1} HNO_3 at high current density (j = 50 kA m^{-2}). The generated vapours were evacuated by pumping and trapped in a sodium hydroxide solution. The concentration of nitric acid was adjusted every day after concentration control. Anodes (1.8 cm^2 each; 3 of the Ti/Pt-5 μm type from Magneto, and

3 of the Nb/BDD type from Condias) were subjected to tests up to their deactivation. It was considered that anodes were deactivated when the cell potential exceeded 10 V [17]. The variation of the cell voltage as a function of time for the 6 tested anodes are reported and discussed in this paper.

3 Experimental results and discussion

3.1 Mass transfer rate

Under industrial conditions, concentration of chloride ions in nitric acid can reach 1 mol L^{-1} [9, 10] whereas for the dechlorination process the final concentration should be lower than 10^{-3} mol L^{-1} to avoid AgCl precipitation when $AgNO_3$ is introduced. The rate of reaction (1) may be controlled by charge transfer or mass transport depending on the applied current density, chloride concentration, and hydrodynamic conditions which may depend on the rate of gas evolution at the anode [11]. If a sufficient potential, or current intensity, is applied to operate reaction (1) by mass transport control, the reaction rate can then be identified to the limiting current I_{lim} corresponding to the maximum reaction rate:

$$I_{lim} = nFSk[Cl^-], \quad (2)$$

where n is the number of electrons exchanged ($n = 1$), F the Faraday constant (96,498 C mol^{-1}), S the electrode surface (m^2) and $[Cl^-]$ the chloride concentration (mol m^{-3}).

The mass transfer coefficient, k, was measured at 60 °C for dechlorination in the tubular reactor under anolyte recirculation at a flow rate $\emptyset = 20$ L min^{-1} consistent with industrial conditions. Measurements were carried out in 6 mol L^{-1} nitric acid with sodium chloride at initial concentration of 0.040 or 0.050 mol L^{-1}, lower than that used typically in the industrial process ($[Cl^-]_0 = 0.1$ mol L^{-1}) in order to obtain current potential curves presenting a net diffusion plateau. Figure 2 presents plots obtained point by point under galvanostatic conditions for electro-oxidation of chloride. For successive controlled current intensity values the electrode potential was registered after 3 s. Chloride oxidation appears distinctly before water discharge as a short plateau of 150 mV length. By operating under these conditions the values of the anode potential are very stable and the I E curve is reproducible. The mass transfer coefficient k was then determined using the limiting current intensity measured at 1.45 V/SCE on Ti/Pt, and 2.5 V on Nb/BDD. Current intensities were corrected by the residual current [18] measured in nitric acid at 6 mol L^{-1}. The mass transfer coefficient k, measured at 60 °C, was equal to 6.01×10^{-5} m s^{-1} at the Ti/Pt 5 µm anode, whereas it was equal to 4.84×10^{-5} m s^{-1} at the Nb/BDD anode. The discrepancy between the two values of k results probably from different induced hydrodynamic conditions established by the different mesh size of the expanded metals. Values of k were used to calculate the $[Cl^-] = f(t)$ curves (Eqs. 5 6).

In the case of silver(I) anodic oxidation the mass transfer coefficient k was measured in the tubular reactor at 30 °C for different flow rates Φ (from 3.5 to 20 L min^{-1}) for two anodes of the same geometric surface $S = 521$ cm^2. Steady-state polarisation curves (not shown) were obtained under galvanostatic conditions at different flow rates for the tubular reactor. Silver(I) oxidation appears distinctly before water discharge; the oxidation wave of silver(I) presents the classic shape of the progressive change of the kinetic limitation from charge transfer to mass transfer with increasing potential [11]. The mass transfer coefficient was determined using the limiting current measured at 2.04 and 2.36 V (vs. SHE) for Ti/Pt and Nb/BDD respectively.

Linear regression of k values (m s^{-1}) as function of Φ (L min^{-1}) conducts to the following correlations:

$$k \times 10^6(\mathrm{Ti/Pt}) = 1.78\,\Phi + 14.72 \quad (3)$$

$$k \times 10^6(\mathrm{Nb/BDD}) = 1.962\,\Phi + 0.1596 \quad (4)$$

For a flow rate of 20 L min^{-1} (mean linear flow rate in the anodic compartment v = 0.3 m s^{-1}) the values of

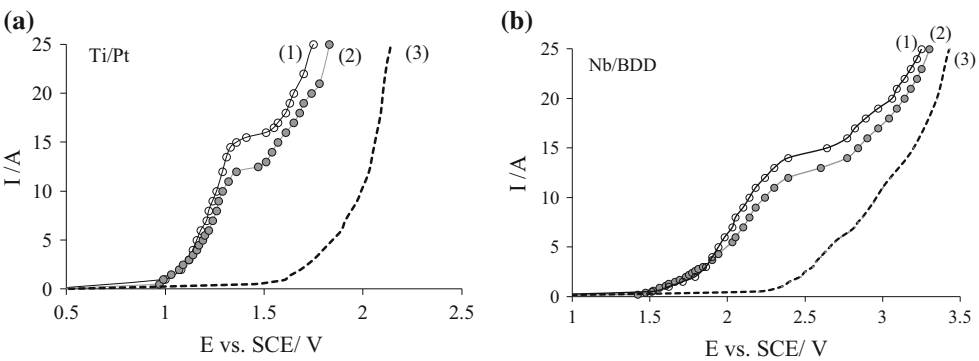

Fig. 2 Current potential curves for Cl^- oxidation on Ti/Pt and Nb/BDD anodes in 6 mol L^{-1} HNO_3; S 521 cm^2. *1* [Cl^-] 0.050 mol L^{-1}; *2* [Cl^-] 0.040 mol L^{-1}; *3* ground current in [HNO_3] 6 mol L^{-1}; T 60 °C; flow rate Φ 20 L min^{-1}

k are: 5×10^{-5} and 4×10^{-5} m s^{-1} for the Ti/Pt and Nb/BDD anodes respectively.

3.2 Dechlorination

Dechlorination experiments were conducted under galvanostatic conditions at applied current intensity equal or higher than the initial limiting current intensity $\left(\alpha = \frac{I}{I^0_{lim}} \geq 1\right)$ for two values of the ratio of the anode surface on the anolyte volume $\left(\frac{S}{V_{sol}}\right)$. When $\alpha = 1$ (at $t = 0$), the process is mass transfer limited and the chloride concentration varies as [18]:

$$C(t) = C_0 \exp\left(-\frac{t}{\tau}\right) \quad (5)$$

where:

$$\tau = V_{sol}/(Sk) \quad (6)$$

Equations 5 and 6 show that the higher the value of the S/V_{sol} ratio is, the shorter is the duration of electrolysis.

Figure 3a shows that 6 mol L^{-1} nitric acid solutions, initially containing 0.1 mol L^{-1} of chloride, can be dechlorinated until 10^{-3} mol L^{-1} on the Ti/Pt anode in around 2500 s at a current intensity ($I = 30$ A) equal to the initial limiting current I^0_{lim} ($\alpha = 1$) at $t = 0$. For the same operating conditions: configuration of the tubular reactor ($S/V_{sol} = 35$ m^{-1}) and galvanostatic conditions ($\alpha = 1$) Fig. 3b (curve I) shows that with a Nb/BDD anode chlorides can be removed in 3000 s. According to the value of the mass transfer coefficient of these two electrodes, electrolysis durations to reach the final chloride concentration of 10^{-3} mol L^{-1} were slightly higher for the Nb/BDD anode than for Ti/Pt. As expected, with a surface electrode reduced by half ($S/V_{sol} = 17.4$ m^{-1}) and an increasing of the ratio α to 2.47 have no accelerating effect (Fig. 3b, curve II). The dotted lines presented in Fig. 3 calculated with Eq. (5) fit correctly with experimental results in accordance with a limitation by mass transfer ($\alpha \geq 1$).

All electrolyses were followed by ionic chromatography in order to detect the eventual formation of chlorate and perchlorate. As the detection limit of the technique was evaluated around 1 ppm for these two oxyanions because of the high concentration of nitric acid (0.06 M, after dilution of the samples by a factor 100) it can be assumed that the concentration of these undesirable anions were (if they are present) at concentration lower than 100 ppm (i.e. $\leq$1 mM).

In summary, in this device characterized by a ratio $S/V_{sol} = 35$ m^{-1}, electrochemical dechlorination can be performed satisfactorily in less than 50 min under standard and safe industrial conditions; therefore, the process carried out with the Nb/BDD could be adapted for industrial application.

3.3 Silver(I) oxidation

In the anodic compartment, Ag(II) generated in aqueous nitric acid solution at 6 mol L^{-1} is stabilized by nitrate ion; thus in the absence of a reducing agent, silver(II) is present as a dark brown nitrate complex [6]:

$$Ag^+ + NO_3 \rightarrow Ag(NO_3)^+ + e \quad (7)$$

However, the increase of the Ag(II) concentration gives a rise to the rate of oxidation of the water according to reaction:

$$2\,Ag(NO_3)^+ + H_2O \rightarrow 2\,Ag^+ + 2\,HNO_3 + {}^1/_2\,O_2 \quad (8)$$

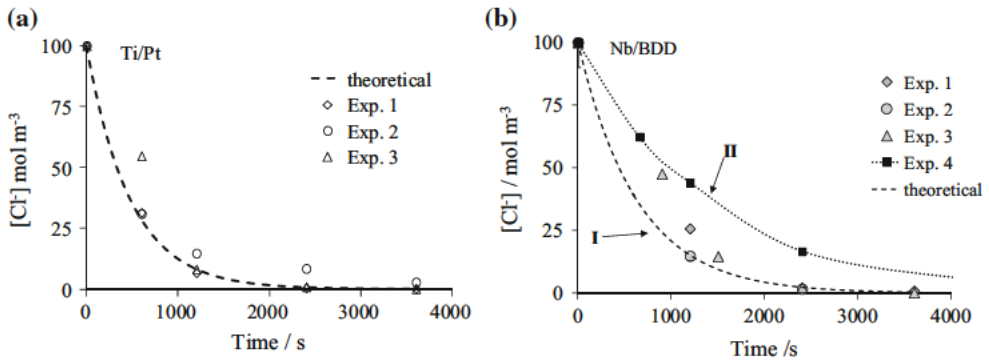

Fig. 3 Calculated (*dotted lines*) and experimental (*symbols*) [Cl$^-$] f(t) curves on **a** Ti/Pt, and **b** Nb/BDD anodes. V_{sol} (anolyte) 1.5 L; $[NaCl]_0$ 0.1 mol L^{-1} in 6 mol L^{-1} HNO_3; T 60 °C; flow rate Φ 20 L min^{-1}; I 30 A. Modelling using **a** k 6.01×10^{-5} m s^{-1} and α 1 for Ti/Pt (S 521 cm^2; I^0_{lim} 30 A), and **b** k 4.84×10^{-5} m s^{-1} for Nb/BDD. Exp. 1 3 (*curve I*): anode surface S 521 cm^2; α 1.23; I^0_{lim} 24.3 A. Exp. 4 (*curve II*): anode surface S 260.5 cm^2 (anode made with 4 rectangular plates); α 2.47; I^0_{lim} 12.2 A

Thus, the concentration of Ag(II) reaches a quasi-stationary value [11].

Referring to a batch recirculation reactor system, the model is based on the mass balance in which the actual rate of Ag(II) generation is expressed as the difference between the production rate R_{gen} by electrolysis and the destruction rate by reaction with water R_{H_2O}:

$$\frac{d[Ag(II)]}{dt} = R_{gen} - R_{H_2O} \tag{9}$$

The rate of Ag(II) production (mol s^{-1} L^{-1}) is given by:

$$R_{gen} = \frac{j_{Ag}S}{nFV_{sol}}, \tag{10}$$

where j_{Ag} is the part of the current density used to generate Ag(II); in a first approximation the volume of the electrochemical reactor is considered as small (around 60 mL) with regard to the total volume of the anolyte ($V_{sol} = 1.5$ L).

The kinetic law of the chemical reaction (8) in nitric acid [11, 19, 20] involves Ag(II) and Ag(I) concentrations as follows:

$$R_{H_2O} = k_{H_2O}\frac{[Ag(II)]^2}{[Ag(I)]} \tag{11}$$

Some values of k_{H_2O} are compiled in [11]. k_{H_2O} depends on the temperature and has been determined experimentally by following the temporal decrease of [Ag(II)] at different temperatures. In the range of 20 35 °C, one obtains:

$$Lnk_{H_2O} = -\frac{11696}{T(K)} + 32.96 \tag{12}$$

For a constant current intensity I higher than the initial limiting current, the partial current $j_{Ag}S$ is calculated by Eq. (2) applied to the anodic oxidation of Ag(I). In this case, the generation rate of Ag(II) is expressed by Eq. (13):

$$\frac{d[Ag(II)]}{dt} = \frac{kS[Ag(I)]}{V_{sol}} - k_{H_2O}\frac{[Ag(II)]^2}{[Ag(I)]} \tag{13}$$

Simulations have been performed by numerically solving Eq. (13) using a finite difference method.

Table 1 shows experimental values of the initial speed of generation of Ag(II) for three current intensities as well as the corresponding conversion of Ag(I) at the stationary state. The Nb/BDD electrode presents performance slightly lower than that of the Ti/Pt electrode for the two highest currents (15 and 30 A). For a current intensity lower than 15 A, the generation rates of Ag(II) obtained with Nb/BDD are similar than those obtained with Ti/Pt.

Results presented in Table 1 show that an increase in the current intensity for the Ti/Pt anode at a value upper than the limiting current increases frankly the rate of silver(II) generation, whereas this rate decreases for the same change in current intensity (15 30 A) in the case of the Nb/BDD anode. This discrepancy suggests that, in the case of the BDD electrode, competitive reactions may happen for $I > I_{lim}$ (see below Eqs. 14 17). Accordingly, using a BDD anode needs a perfect control of the current to optimise Ag(II) generation.

Figure 4a, b shows experimental results (points) for galvanostatic electrolyses performed in the tubular reactor. The experimental stationary Ag(II) concentration is slightly higher for Ti/Pt than for Nb/BDD (19 and 17 mol m^{-3} respectively); in accordance with numerical values of the mass transfer coefficient evaluated for the two materials [Eqs. (3) and (4)], the production rate R_{gen} in Eqs. 9 and 13 is higher for the Ti/Pt anode. Figure 4 shows also the simulation of Ag(II) concentration variation (curves) during the transient and stationary periods of electrolysis. It is seen that the simple model described by Eq. (13) fits better for Ti/Pt (difference less than 2 %) than for Nb/BDD (difference around 10 %). In fact, if the electrolyses started under conditions for which α was 1.2 and 1.5 for Ti/Pt and Nb/BDD respectively, at the stationary state α reached values around 1.9 and 2.3 respectively, what implies oxygen evolution on Pt whereas on BDD a more complex mechanism may be expected, according to Eqs. (14) (17) [21 23]:

$$H_2O \rightarrow {}^{\bullet}OH + H^+ + e \tag{14}$$

$$Ag^+ + {}^{\bullet}OH \xrightarrow{K_{15}} Ag^{2+} + OH \tag{15}$$

$${}^{\bullet}OH + {}^{\bullet}OH \xrightarrow{K_{16}} H_2O_2 \tag{16}$$

$$2\ Ag(NO_3)^+ + H_2O_2 \xrightarrow{K_{17}} 2\ Ag^+ + O_2 + 2\ H^+ + 2\ NO_3 \tag{17}$$

Reaction (15) suggested by Barker and Fowles [22] and which corresponds to a fast reaction in water ($k_{15} = 6.3 \times 10^9$ L mol^{-1} s^{-1}) could be favored in concentrated nitric acid because of neutralization of OH^- and complexation of Ag(II) by the high concentration of nitrate. On the opposite, Ag(II) is reduced by another pathway involving hydrogen peroxide easily formed close to the BDD anode ($k_{16} = 5.5 \times 10^9$ L mol^{-1} s^{-1}) [21]. Reaction (17) considered to be pseudo-first order is very fast ($k_{17} = 300$ s^{-1}) and the steady-state concentration of H_2O_2 should be very low [23]. Let us note furthermore that some traces of silver oxide (AgO) formed on the electrode could activate oxygen evolution [24].

In summary, electrochemical generation of silver(II) proceeds on Nb/BDD anode at rate similar to that on the Ti/Pt anode; however, the process is complicated by side reactions implying the chemical reduction by water (Eq. 8) and by hydrogen peroxide generation in the case where

Table 1 Experimental values of Ag(II) generation rate and conversion at stationary state as functions of current intensity for Nb/BBD and Ti/Pt anodes in the tubular reactor. $[Ag(I)]_0$ 0.05 mol L^{-1}, $[HNO_3]$ 6 mol L^{-1}, T 30 °C, Ø 20 L min^{-1}, S 521 cm^2. Limiting current intensity: 9.9 A (Nb/BDD); 12.6 A (Ti/Pt)

Current/A	Nb/BDD		Ti/Pt 5 µm	
	Generation rate mol m^{-2} min^{-1}	Conversion %	Generation rate mol m^{-2} min^{-1}	Conversion %
7.3	5.99×10^{-2}	34.4	6.19×10^{-2}	36.83
15	7.31×10^{-2}	33.04	9.36×10^{-2}	41.82
30	6.59×10^{-2}	[a]	1.29×10^{-1}	[a]

[a] Due to excessive heat release the temperature of the electrolyte increased too much to measure accurately the conversion

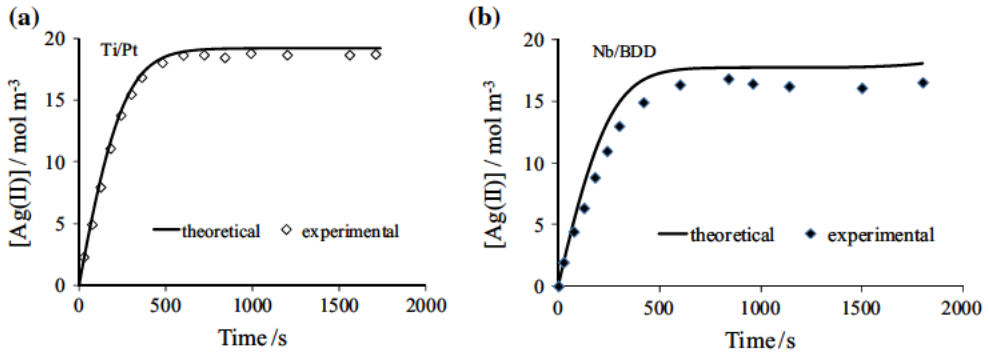

Fig. 4 Theoretical (*line*) and experimental (*symbol*) variation of Ag(II) concentration during electrolysis. Conditions: $[Ag(I)]_0$ 0.05 mol L^{-1}; T 30 °C; $[HNO_3]$ 6 mol L^{-1}; I 15 A, k_{H2O} 3.54×10^{-3} s^{-1}. **a** Anode Ti/Pt: k 5×10^{-5} m s^{-1}. **b** Anode Nb/BDD: k 4.24×10^{-5} m s^{-1}

BDD anode is submitted to a current higher than the mass transfer limiting current.

3.4 Electrode stability

The service life of an electrode material is a mattering parameter to estimate its time of use and validate its industrialization. It has been shown that diamond electrodes are etched electrochemically under certain experimental conditions [25 and ref. therein]. The mechanisms that can cause diamond film corrosion or detachment are complex [17]. Chen et al. [26] tested boron-doped diamond films at 5 kA m^{-2} in a solution of 1.0 mol L^{-1} HNO_3 + 2.0 mol L^{-1} NaCl; their experiments show that no severe microstructural or morphological damage after periods of time up to 20 h. Thus, it was important to test a series of samples of Ti/Pt 5 mm and Nb/BDD under the real conditions of use. For a first evaluation accelerated life tests were conducted.

Figure 5 shows the variation of the cell potential during electrolysis under very high anodic current density (50 kA m^{-2}) for six electrodes. The relative jump of potential indicates the total deactivation of an electrode. The lifetime of three Ti/Pt anodes were respectively of 880, 1280 and 1550 h whereas those of the diamond anodes were 1620, 1720 and >1810 h. A theoretical extrapolation based on a practical current density of 1500 A m^{-2} leads to a minimal life expectancy of more than 3 years for Ti/Pt (value in agreement with the industrial experience on the Ti/Pt) and approximately 6 years for Nb/BDD.

4 Conclusions

This study performed with a tubular electrochemical cell has shown that the Nb/BDD anode represents an interesting alternative to the Ti/Pt anode for the dechlorination as well as for the regeneration of Ag(II) in nitric acid solution. It is possible to run the two steps sequentially in the same reactor using Nb/BDD anodes, as has been shown for Pt/Ti anodes. Results obtained with Ti/Pt 5 µm and Nb/BDD anodes were satisfactory since dechlorination reached 99 %, value in accordance with the practical objective. Furthermore, the formation of oxyanions of chlorine was not detected during electrochemical dechlorination. The specific particularity of the Nb/BDD electrode lies in the

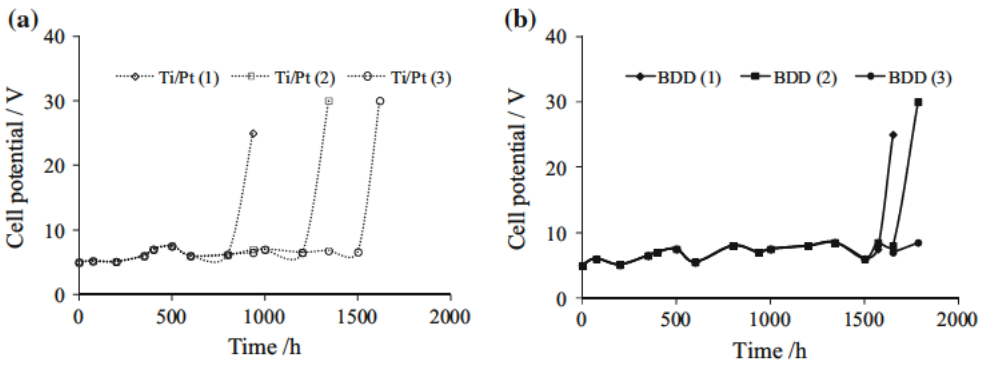

Fig. 5 Accelerated life tests of **a** Ti/Pt anodes and **b** BDD anodes in 6 mol L^{-1} HNO_3 solution for I 50 kA m^{-2} at 30 °C

service life practically double than that of Ti/Pt. Monitoring the rate of Ag(I) oxidation on the BDD anode imposes however the current density to be controlled to avoid the generation of hydroxyl radicals susceptible to slow down the rate of the Ag(II) electrochemical regeneration via hydrogen peroxide formation.

References

1. Ryan JL, Bray LA, Wheelwright EJ, Bryan GH (1990) Catalyzed electrolytic plutonium oxide dissolution (CEPOD The past sev enteen years and future potential). In: Proceedings on interna tional symposium to communication 50th anniversary of transuranium elements, Washington, DC, 26 31 Aug 1990
2. Ryan JL, Bray LA, Boldt AL (1987) Dissolution of PuO_2 or NpO_2 using electrolytically regenerated reagents. US Patent 4,686,019
3. Koehly G, Bourges J, Madic C, Lecomte M (1988) Process for the recovery of plutonium contained in solid waste. US Patent 4,749,519
4. Bourges J, Madic C, Koehly G, Lecomte M (1986) Dissolution du bioxyde de plutonium en milieu nitrique par l'argent(II) élec trogénéré. J Less Common Met 122:303 311
5. Zundelevich Y (1992) The mediated electrochemical dissolution of plutonium oxide: kinetics and mechanism. J Alloys Compd 182:115 130
6. Steele DF (1990) Electrochemical destruction of toxic organic industrial waste. Platin Metals Rev 34:10 14
7. Steele DF (1990) Regeneration of nitrous acid by oxidation with direct application of heated nitric acid. US Patent 4,925,643
8. Brossard M P, Belmont J M, Baron P, Blanc P, Broudic J C (2003) Dechlorination, dissolution, and purification of weapon grade plutonium oxide contaminated with chlorides: tests per formed in the CEA Atalante facility for the aqueous polishing part of MOX fuel fabrication facility. Proc Glob 2003:485 491
9. Pierce RA, Campbell Kelly RP, Visser AE, Laurinat JE (2007) Removal of chloride from acidic solutions using NO_2. Ind Eng Chem Res 46:2372 2376
10. Koehly G, Madic C, Saulze J L (1989) Process for eliminating the chloride ions present in contaminated solid wastes, such as incineration ashes contaminated by actinides. US Patent 4,869,794
11. Racaud C, Savall A, Rondet Ph, Bertrand N, Groenen Serrano K (2012) New electrodes for silver(II) electrogeneration: compar ison between Ti/Pt, Nb/Pt, and Nb/BDD. Chem Eng J 211 212:53 59
12. Ferro CS, de Battisti A, Duo I, Comninellis Ch, Haenni W, Perret A (2000) Chlorine evolution at highly boron doped diamond thin film electrodes. J Electrochem Soc 147:2614 2619
13. Polcaro AM, Vacca A, Mascia M, Palmas S, Rodiguez Ruiz J (2009) Electrochemical treatment of waters with BDD anodes: kinetics of the reactions involving chlorides. J Appl Electrochem 39:2083 2092
14. Bergmann MEH, Rollin J, Iourtchouk T (2003) The occurrence of perchlorate during drinking water electrolysis using BDD anodes. Electrochim Acta 54:2102 2107
15. Sanchez Carretero A, Saez C, Canizares P, Rodrigo MA (2011) Electrochemical production of perchlorates using conductive diamond electrolyses. Chem Eng J 166:710 714
16. Lange R, Maisonhaute E, Robin R, Vivier V (2013) On the ki netics of the nitrate reduction in concentrated nitric acid. Elec trochem Comm 29:25 28
17. Kraft A (2007) Doped diamond: a compact review on a new, versatile electrode material. Int J Electrochem Sci 2:355 385
18. Walsh F (1993) A first course in electrochemical engineering (Ch. 6). The Electrochemical Consultancy (Romsey) Ltd, Romsey
19. Po HN, Swinehart JH, Allen TL (1968) The kinetics and mechanism of the oxidation of water by Ag(II) in concentrated nitric acid solution. Inorg Chem 7:244 249
20. Lehmani A, Turq P, Simonin JP (1996) Oxidation of water and organic compounds by silver(II) using a potentiometric method. J Electrochem Soc 143:1860 1865
21. Kapałka A, Fóti G, Comninellis Ch (2009) The importance of electrode material in environmental electrochemistry. Formation and reactivity of free hydroxyl radicals on boron doped diamond electrodes. Electrochim Acta 54:2018 2023
22. Barker GC, Fowles P (1970) Pulse radiolytic induced transient electrical conductance in liquid solutions. Part 3 Radiolysis of aqueous solutions of some inorganic systems. Trans Faraday Soc 66:1661 1669
23. Rance PJW, Nikitina GP, Korolev VA, Kirshin MYu, Listopadov AA, Egorova VP (2003) Features of electrolysis of nitric acid solutions of silver: I. Behavior of Ag(II) in HNO_3 solutions. Radiochemistry 45:346 352
24. Panizza M, Duo I, Michaud P A, Cerisola G, Comninellis Ch (2000) Electrochemical generation of silver(II) at boron doped diamond electrodes. Electrochem Solid State Lett 3:550 551
25. Chaplin BP, Hubler DK, Farrell J (2011) Understanding anodic wear at boron doped diamond film electrodes. Electrochim Acta 89:122 131
26. Chen Q, Granger MC, Lister TE, Swain GM (1997) Morpho logical and microstructural stability of boron doped diamond thin film electrodes in an acidic chloride medium at high anodic current densities. J Electrochem Soc 144:3806 3812